J Nanopart Res (2020) 22: 279
https://doi.org/10.1007/s11051-020-05006-2

RESEARCH PAPER

Selective functionalization of the outer surface of MCM-48-type mesoporous silica nanoparticles at room temperature

Shewaye Yismaw · Stefan G. Ebbinghaus · Marianne Wenzel · David Poppitz · Roger Gläser · Jörg Matysik · Frank Bauer · Dirk Enke

Received: 7 April 2020 / Accepted: 1 September 2020 / Published online: 11 September 2020

Abstract In this study, a suitable route for the selective functionalization of the outer surface of MCM-48-type mesoporous silica nanoparticles (MSNs) and its impact on the physicochemical properties were investigated. The synthesis of MCM-48 nanoparticles with intact cubic ordered mesopore structure and functionalized outer particle surface was managed by postsynthetic and co-condensation modification routes with 3-methacryloxypropyltrimethoxy-silane (MPS). The results of FTIR, ^{29}Si and ^{13}C NMR, thermogravimetric, and elemental analysis confirmed the successful silane surface grafting by both methods. The nitrogen sorption analysis showed the selective outer surface functionalization by the postsynthetic route for the synthesized MCM-48 nanoparticles containing the template still inside the pore channels and in the case of the co-condensation route via late addition of the silane precursors into the synthesis batch containing a fully grown silica. The solvent type in the former approach and silane addition time during the particle growth in the later route showed a significant impact on the silane content and site selective binding. The amount of grafted silane was determined by thermogravimetric and elemental analysis. It was found to increase using toluene in the postsynthetic modification route. The average particle size measured from SEM/TEM analysis ranges from 290 to 350 nm. The cubic ordered pore structure of the final silane grafted MSNs was fully preserved in both functionalization routes as corroborated from XRD analysis. In conclusion, MCM-48 nanoparticles selectively functionalized on the outer particle surface are favorable candidates for the subsequent site selective grafting reactions.

Keywords Outer surface functionalization · MCM-48 mesoporous silica nanoparticles · Organosilane grafting · Co-condensation · Solvent effect

S. Yismaw · D. Poppitz · R. Gläser · F. Bauer · D. Enke (✉)
Institute of Chemical Technology, Universität Leipzig, Linnéstraße 3 04103 Leipzig Germany
e-mail: dirk.enke@uni-leipzig.de

S. Yismaw
Department of Chemistry, University of Gondar, P.O. Box 196 Gondar Ethiopia

S. G. Ebbinghaus
Institute of Chemistry, Martin-Luther-Universität Halle-Wittenberg, Kurt-Mothes-Straße 2 06120 Halle (Saale) Germany

M. Wenzel · J. Matysik
Institute of Analytical Chemistry, Universität Leipzig, Linnéstraße 3 04103 Leipzig Germany

Introduction

Immobilization of reactive organic functional groups on oxide supports such as mesoporous silica nanoparticles (MSNs) has become a preliminary activity for applications in drug delivery (Morelli et al. 2011; Tarn et al. 2013; Vashist et al. 2014), catalysis (Zamboulis et al. 2010; Léonard et al. 2011), bioimaging (Wang et al. 2013; Biju 2014), bioseparation (Tang et al. 2013),

optics (Feng and Zhang 2013), and polymer brushes (Hui et al. 2014). To use MSNs as host materials for biomedical applications, the surface chemistry plays a great role besides its particle size, morphology, textural properties, and pore structures (Chang et al. 2011; Bouchoucha et al. 2016). Moreover, in functional MSNs, the inorganic silica offers excellent textural properties including large specific surface area, high pore volume and narrow pore width distribution, and good mechanical and thermal stability. The integrated organic part provides ductility, flexibility, and chemical functionality either for direct use or for subsequent modification with other organic materials like polymers (Trewyn et al. 2007; He et al. 2010; Mamaeva et al. 2013).

Organosilanes (R-Si(OR′)$_3$) containing hydrolysable (R′; methoxy or ethoxy groups) and reactive organic functional groups (R; methacryloxy, amino, epoxy, mercapto, vinyl groups, and so on) in the structure have been widely used to modify the silica surface (Bauer et al. 2002; Sun et al. 2005; Chen et al. 2007). Commonly, these organic moieties can be introduced to the silica surface either via a multi-step postsynthetic functionalization or via one-step direct co-condensation methods (Luan et al. 2005; Marini et al. 2008). Postsynthetic functionalization can be conducted using already synthesized MSNs after either removal of pore generating agent or with its presence inside the pore channels (Tsai et al. 2009; Morelli et al. 2011). This can be realized because of the large number of surface silanol groups that undergo direct condensation with organosilanes and/or the hydrolysis/self-condensation of the alkoxy groups of silanes due to the physisorbed water resulting in subsequent condensation on the silica surface. In the co-condensation method, the functionalized MSNs can be obtained through adding the silane precursor bearing the desired functional group to the batch of synthesis reaction composition including the silica precursor, organic template, and others. The direct co-condensation approach merges multiple steps of synthesis and functionalization and helps to efficiently control the site selective distribution of the organic groups (Kecht et al. 2008; Morelli et al. 2011; Effati and Pourabbas 2012; Khosraviyan et al. 2016).

The location of the organic moieties either can be restricted inside the mesopores, on the particle outer surface, or homogenously distributed on both sites during the synthesis of mesoporous silica-organic composite materials depending on the desired applications. Kecht et al. (2008) summarized the role of selective functionalization of the outer surface of silica nanoparticles for many applications: (i) it determines colloidal stability and interaction with the surrounding environment, (ii) it does not influence the diffusion of the guest molecules into the mesopores, and (iii) it allows attachment of large molecular moieties keeping the internal textural properties intact. Nevertheless, exclusive site selective surface functionalization of different types of MSNs remains as a challenge for researchers over the years (Kecht et al. 2008; Morelli et al. 2011; Effati and Pourabbas 2012; Khosraviyan et al. 2016). In some drug delivery applications using MSNs as reservoir, selective modification of the external surface with optimal textural properties of the nanoparticles is required to fully access the inner pore wall of the as-synthesized material for guest molecule loading (Morelli et al. 2011; Wei et al. 2012; Jin et al. 2017).

To the best of our knowledge, no previous investigations have been published on the synthesis of selective outer surface functionalized MCM-48-type mesoporous silica nanoparticles particularly using a one-pot synthesis method. In this study, we present the successful synthesis of MCM-48 silica nanoparticles functionalized on the outer surface with intact ordered pore structure and morphological properties in site selective manner via the systematic application of postsynthetic grafting and co-condensation approaches. In both modification routes, the undesirable functionalization of the inner pore surface could be inhibited by choosing suitable reaction conditions and their efficiency for the selective outer particle surface functionalization was compared. In the present contribution, the influence of surface modification routes and the type of solvent on the site selective functionalization, content of acrylate functional groups, ordered pore structure, and textural properties of MCM-48-type silica nanoparticle were comprehensively investigated. 3-methacryloxypropyltrimethoxy-silane (MPS), having a favorable functional group important for further chemical grafting of other moieties (polymers), was chosen for both modification routes. The functional groups on the outer surface of the particle define the later site selective (outer surface) chemical grafting processes of polymers without affecting the textural properties of the core silica. Therefore, the experimental details of selective functionalization of the outer surface of silica particles are crucial preliminary steps for the subsequent polymer grafting process

and intended future application of this composite material. This work involves the synthesis, selective functionalization of the outer surface, and detailed characterization of MCM-48 structured MSNs.

Experimental

Chemicals

Tetraethyl orthosilicate (TEOS, 99%) and 3-methacryloxypropyltrimethoxy-silane (MPS, 98%) were purchased from ABCR (Karlsruhe, Germany). Absolute ethanol (EtOH, 100%), toluene (100%) and ammonia hydroxide solution (NH_3OH, 25 wt%) were received from VWR Chemicals (Darmstadt, Germany). Triethanolamine (TEA, 99%) was delivered by Acros organics (Geel, Belgium), cetyltrimethylammonium bromide (CTAB, 99%) by Sigma-Aldrich (Steinheim, Germany), and ammonium nitrate (NH_4NO_3, 99%) by VWR Chemicals (Leuven, Belgium). All chemicals were used as received without any further purification. Deionized water was used for all experiments.

Synthesis of functionalized MCM-48 nanoparticles

The two different functionalization routes based on postsynthetic grafting and co-condensation processes were investigated and compared in this study. To address selective functionalization of the outer surface in the multi-step postsynthetic process, cubic mesophase structure (MCM-48) MSNs with particle diameter around 295 nm were synthesized according to our previously published procedure (Yismaw et al. 2019) with a molar ratio of 1 TEOS:0.15 CTAB:32 NH_3OH:598 H_2O:79 C_2H_5OH:11 TEA in the synthesis mixture. The synthesized MSNs containing CTAB as a template inside the pore channels were separated by centrifugation, washed, and dried overnight at 120 °C. The dried material was redispersed into 100 mL absolute ethanol or anhydrous toluene and subjected for modification via adding MPS (4.23 mmol g^{-1}) on the fresh MCM-48 sample (expecting silane grafting density of about 2 molecules nm^{-2} calculated based on total specific surface area of 1229 $m^2\ g^{-1}$). The reaction was carried out without any catalyst or water at room temperature under stirring for 17 h (Kecht et al. 2008; Florea et al. 2013). The silane-modified MSNs were collected by centrifugation and washed repeatedly with ethanol. However, under anhydrous conditions, the alkoxy groups of the silane (–O–CH_3) will not only react with the hydroxyl groups on the silica surface via a direct condensation mechanism but unfortunately will also undergo separate hydrolysis/condensation steps with traces of water efficiently physisorbed on the hydrophilic silica surface. In the current study, to accomplish the binding of the silanes preferentially on the outer silica surface with intact desired MCM-48 properties, the modification was performed before surfactant removal at room temperature (Fig. 1a).

Alternatively, the reactants were mixed in the co-condensation route following the general synthesis composition and procedure for MSNs as described before. Moreover, the organosilane precursor was directly incorporated into the batch of MSNs reaction composition following colloidal silica formation at specific time periods of ageing (Fig. 1b). The time of silane precursor addition was varied from 5 to 10, 20, and 35 min of ageing after the silica precursor TEOS addition into aqueous basic media (pH 11). Keeping the other reaction conditions constant, the silane was added at once to the mixture:

1). During the growth of the particles after 5 (MM-Co_5), 10 (MM-Co_{10}), and 20 (MM-Co_{20}) minutes of ageing. The reaction was continued for further 35 min under stirring in all cases.
2). To a completely grown material (after 35 min of ageing) (MM-Co_{35}) and stirred mildly (500 rpm) for additional 20 min.

All reactions were carried out at room temperature. The trialkoxysilanes are rapidly hydrolyzing into anionic species, whereas the non-polar micelles chains inside the channels prevent their diffusion into the pores. The hydrolysis of the silane methoxy (–O–CH_3) groups into silanol species in the batch of reaction mixture under basic aqueous conditions causes its further condensation with silanols of neighboring organosilane molecules and/or the silica surface hydroxyl groups (Florea et al. 2013; Bauer et al. 2017). This can assist selective functionalization of the outer surface during the silica framework formation of the growing particle via hydrolysis and subsequent condensation (Fig. 1b). Moreover, in the present study, it was proposed that the co-condensation approach, via the late addition of the silane precursor to the reaction mixture containing fully grown silica particles, selectively modifies the outer surface

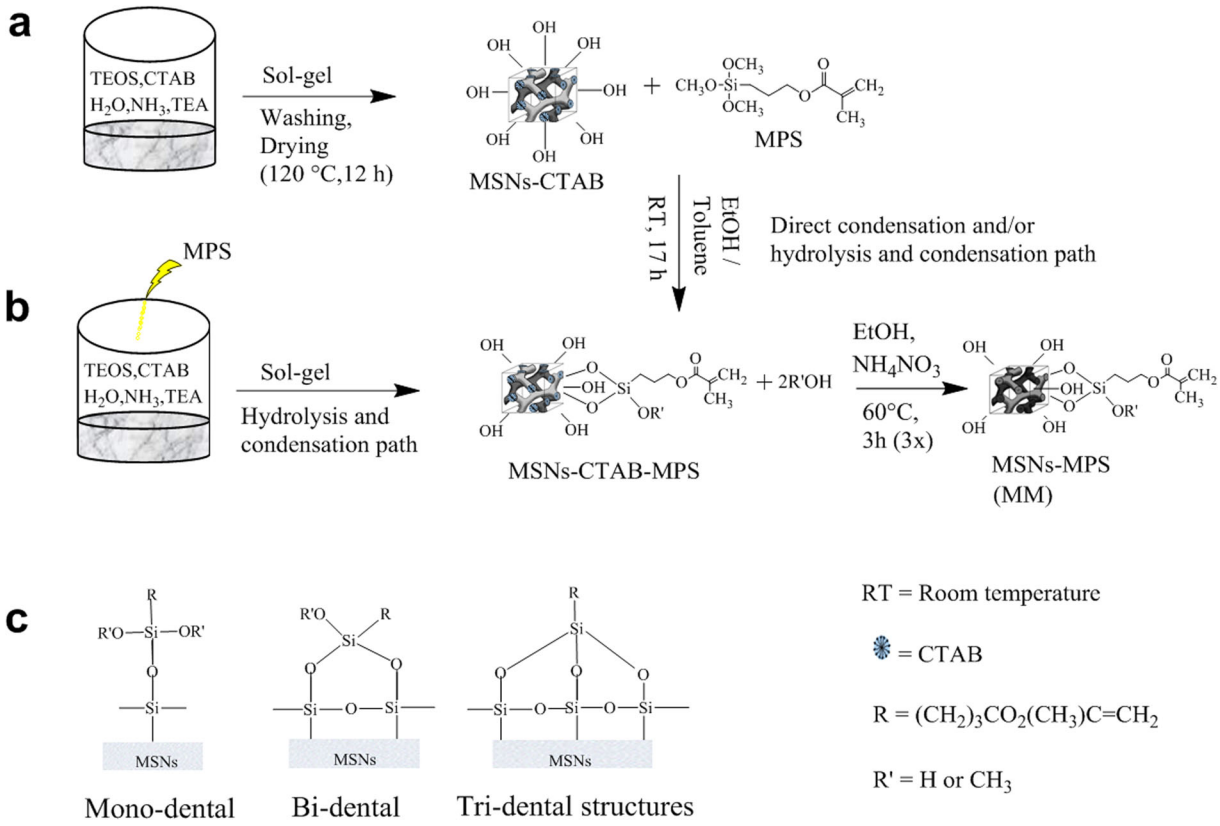

Fig. 1 Reaction scheme demonstrating (**a**) the postsynthetic and (**b**) co-condensation routes for the proposed site selective silica surface modification. (**c**) Modes of silane binding to the silica surface determined by ^{29}Si NMR

instead of homogenous distribution as well inside the pores and pore entrance.

Afterwards, the functionalized material was separated, washed repeatedly, and dried at 80 °C under vacuum. Finally, the template was removed from the mesoporous channels by solvent extraction process in both methods (Yismaw et al. 2019). The acrylate functionalized materials (designated as MSNs-MPS or MM) were dried under vacuum condition at 80 °C for 24 h. A reaction scheme for selective silane grafting on the outer surface of MCM-48-type MSNs following both modification methods is shown in Fig. 1.

Characterization

A vector 22 ATR-FTIR spectrometer (attenuated total reflectance Fourier transform infrared spectroscopy) (Bruker, Billerica, MA) was used to observe the variation in surface chemistry of silica before and after the functionalization. Both ^{29}Si high-power decoupled (HPDEC) and ^{13}C Cross-polarization (CP) solid-state magic angle spinning nuclear magnetic resonance (MAS NMR) spectra were recorded using a Bruker DRX-400 WB NMR spectrometer (Bruker Biospin, Karlsruhe, Germany) equipped with a 4-mm MAS BB X/^{1}H probe operating at a Larmor frequency of 79.49 MHz for ^{29}Si, 100.62 MHz for ^{13}C, and 400.15 MHz for ^{1}H, respectively. The spectra were acquired at a spinning speed of 12 kHz and a temperature of 20 °C using tetramethylsilane (TMS) at 0 ppm as external reference. For the HPDEC measurements, 512 scans were collected with a $\pi/2$ pulse of 6.75 μs on ^{29}Si and a recycle delay of 60 s. A SW_f-TPPM heteronuclear decoupling was used during the acquisition. For the CP measurements, 1024 scans were accumulated. During the contact time of 2 ms, a linearly ramped pulse was applied to fulfill the Hartmann-Hahn condition for polarization transfer from protons to carbons. The $\pi/2$ pulse was 2.5 μs on ^{1}H, and the recycle delay was set to 5 s. A SW_f-TPPM heteronuclear decoupling was used during the acquisition. The thermal weight losses of samples were measured by thermogravimetric analysis

(TGA) from ambient temperature to 800 °C at a heating rate of 10 °C min^{-1} in a stream of air using a STA 409 thermobalance (Netzsch, Selb, Germany). The weight percent of carbon and hydrogen was determined from CHN elemental analysis (Vario EL III, Elementar Analysensysteme, Langenselbold, Germany). The silane grafting density (molecules nm^{-2}) was estimated based on the TG and elemental analysis data (Bartholome et al. 2005; Pardal et al. 2009).

Nitrogen (N_2) physisorption measurements were performed using a Quantachrome Autosorb iQ (Quantachrome, Boynton Beach, FL). Prior to the sorption measurements, all samples were treated under vacuum at 80 °C for 20 h. The specific surface areas (S_{BET}) were calculated using the Brunauer-Emmett-Teller (BET) method in the range of $p/p_0 = 0.05–0.35$, and the total pore volume was obtained at the maximum relative pressure $p/p_0 = 0.98$. The external surface area (S_{ex}) of the as-synthesized MSN sample was measured before surfactant extraction, keeping the pores filled by the template, and calculated using the BET or v-t (DeBoer) method. The non-local density functional theory (NLDFT) method was applied to estimate the pore diameters using the adsorption branch model considering N_2 sorption at − 196 °C in silica with cylindrical pore geometry. The effect of surface modification process on the cubic ordered mesopore structure was determined by low angle powder X-ray diffraction (XRD) on a D8 Advance diffractometer (Bruker AXS, Karlsruhe, Germany) (Cu Kα radiation $\lambda = 1.54$ Å, LynxEye one-dimensional silicon strip detector) in the range $2\theta = 0.4–10.0°$ with a step size of 0.01° and a counting time of 1 s $step^{-1}$. A Leo Gemini 1530 scanning electron microscope (SEM) (Zeiss, Oberkochen, Germany) and JEM2100Plus transmission electron microscopy (TEM) (JEOL, Tokyo, Japan) analyses were used to record the pictures.

Results and discussion

Physicochemical properties of functionalized MCM-48 nanoparticles

FTIR and NMR spectroscopy analyses

The effect of solvent properties on the content of acrylate groups, textural properties, and site of silane binding on the silica surface in the multi-step postsynthetic route was evaluated using absolute ethanol and dry toluene (designated as E and T, respectively, in the text, table and graphs) solvents under the same silica to MPS ratio and identical reaction conditions. FTIR spectra (Fig. 2) showed the surface chemistry of the non-functionalized sample (MSNs) and after treating with MPS using ethanol (MM1E) or toluene (MM1T) solvents. The high intense FTIR peaks for all samples appeared at 1100 and 804 cm^{-1} are associated with the asymmetric and symmetric stretching vibrations of –Si–O–Si– in the silica framework, respectively, and the peak at 970 cm^{-1} is attributed to –Si–OH bending vibrations characteristic for silica (Doadrio et al. 2006; Pinto et al. 2006). A peak at 1638 cm^{-1} was observed after MPS modification due to asymmetric vibrations of vinyl (C=C) groups commonly overlapping with asymmetric vibrations of the moisture on MSNs surface. The intense new peak at around 1723 cm^{-1} was attributed to the carbonyl (C=O) stretching vibration of the acrylate groups grafted on the MSNs surface (Doadrio et al. 2006). This characteristic carbonyl group peak reveals the successful chemical grafting of the silane molecules. FTIR peaks of all samples showed a broad band from 3700 to 3200 cm^{-1} pointing to the stretching OH vibrations of physisorbed water molecules on the silica surface. A peak from 2826 to 3000 cm^{-1} is generated by the aliphatic C–H stretching vibration of the grafted propyl acrylate molecules for the MPS treated samples and certain organic residues for the untreated sample (Al-Oweini and El-Rassy 2009; Subagyono et al. 2014; Perissinotto et al. 2015).

Moreover, the C=O group peak intensity at around 1723 cm^{-1} is higher for a sample modified using toluene (MM1T) compared with ethanol (MM1E) (Fig. 2). This designates the grafting of large number of acrylate groups on the MSNs surface using toluene, which is also supported by TG and elemental analysis results (Table 1). These observations can be interpreted with differences in the solvent properties. Overall, during the modification process, the solvent is used to disperse and transport the silane precursor molecules as well as to solvate the silanol groups on silica surface. The latter modifies the surface acid-base properties and the polarity. Zimmermann et al. (2002) reported that the interaction of high hydrogen-bonding acceptor solvents like ethanol with the silica surface reduces the number of active surface silanol sites that results in a decrease of the catalytic activity of the silica surface for electrophilic reactions. In addition, the ethanol may compete with the

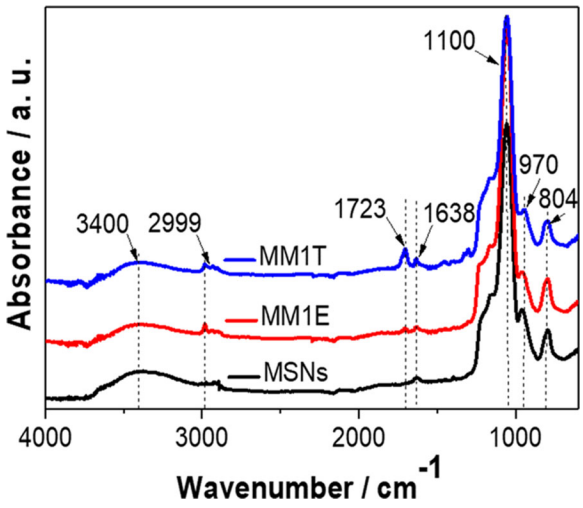

Fig. 2 FTIR spectra of the non-functionalized (MSNs) and MPS surface functionalized samples via postsynthetic route using ethanol (MM1E) or toluene (MM1T)

organosilane molecules for the trace amount of physisorbed water and the surface hydroxyl groups, favoring the formation of small size silane clusters that further bind on silica. Overall, these solvent properties reduce the final grafting amount for a sample prepared using ethanol as a solvent. The result observed in our work is in line with a study of Zhao et al. (2011). The effects described above are weaker for the non-polar solvent toluene, in which the physically adsorbed moisture on the silica surface is immiscible. Hence, silane hydrolysis and self-condensation between the neighboring organosilanes lead to large silane oligomer formation prior to surface grafting (Bauer et al. 2000, 2017). This results in higher acrylate grafting density. In general, the solvent type has a pronounced effect on the organosilane content grafted on the surface.

The chemical grafting of organosilane molecules on the silica surface was further qualitatively evidenced by ^{13}C and ^{29}Si solid-state NMR measurements for selected samples (Fig. 3). The ^{13}C CP-MAS NMR spectrum of MM1T features several resonances confirming the presence of different functional groups with respect to the non-functionalized sample (MSNs) (Fig. 3a). After silane treatment, the signal at 171.8 ppm (h, –C=O) is attributed to the carbonyl group; the signals at 138.7 ppm (g, –C=CH_2) and 128.1 ppm (f, CH_2=C–) are ascribed to the vinyl groups. The signals at 68.0 ppm (e, –O–CH_2–), 24.0 ppm (b, –CH_2–), 18.6 ppm (c, CH_3–C–), and 9.7 ppm (a, –CH_2–Si–) are attributed to the alkane carbons of the silane molecule grafted on the surface (Villenas et al. 2015). The signal at 61.7 ppm indicates the presence of remaining methoxy groups (d, –O–CH_3) and points to incomplete hydrolysis/condensation reactions of MPS under the reaction conditions applied. Likewise, the FTIR and ^{13}C NMR spectra for a sample prepared via the co-condensation method (MM-CO_{35}) are in agreement with MM1T (data not shown).

The ^{29}Si HPDEC-MAS NMR spectra (Fig. 3b) in the range − 90 to − 111 ppm of the non-modified MCM-48 silica (MSNs) and silane-treated (MM1T and MM-Co_{35}) samples bear much structural resemblance. This

Table 1 Characteristics of MCM-48 silica before and after surface modification

Sample	S_{BET} (S_{ex}) (m^2 g^{-1})[a]	V_{meso} (cm^3 g^{-1})[a]	d_{meso} (nm)[a]	Δm (wt%)[b]	X_{TGA} (molecules nm^{-2})[b]	ΔC (wt%)[c]	X_{EA} (molecules nm^{-2})[c]	X_d (nm)[d]
MSNs	1229 (18)	0.85	3.4	3	-	5.1	-	295
MM1E	1093	0.74	3.4	11	16[e]	4.2	16[e]	316
MM1T	981	0.60	3.1	17	31[e]	7.2	29[e]	322
MM-Co_{35}	1013	0.60	3.2	20	39[e]	9.3	40[e]	337
MM-Co_{20}	994	0.50	3.0	-	-	11.4	0.9	328
MM-Co_{10}	978	0.40	3.0	-	-	13.2	1.1	312
MM-Co_5	752	0.33	2.2	-	-	14.6	1.7	318

[a] BET surface area (S_{BET}), external surface area (S_{ex}), mesopore size (d_{meso}), and volume (V_{meso}) based on nitrogen physisorption measurements

[b] Weight loss in the range 200–800 °C (Δm) and grafting density (X_{TGA}) estimated from TGA

[c] Actual carbon content (ΔC) and grafting density (X_{EA}) estimated from elemental analysis

[d] Particle size (X_d) estimated from SEM analysis

[e] Grafting density (X) calculated on basis of the external surface area (S_{ex})

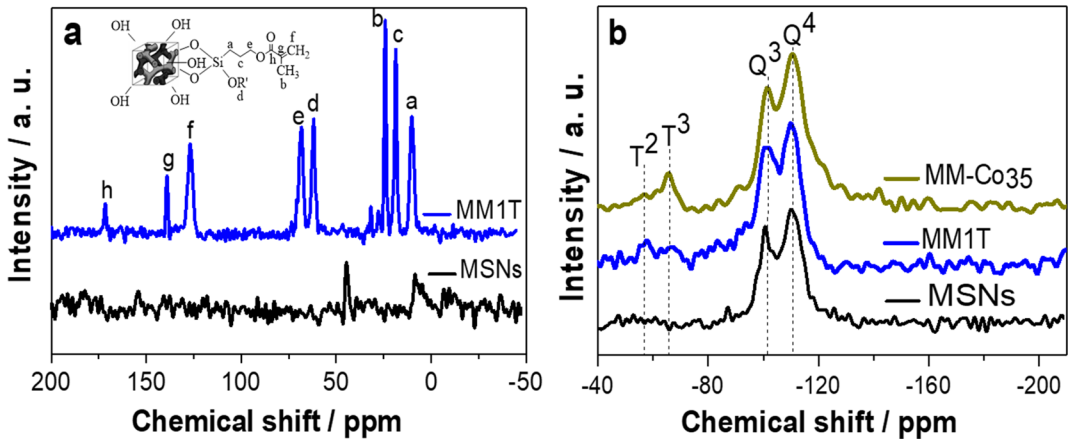

Fig. 3 ^{13}C CP-MAS (**a**) and ^{29}Si HPDEC-MAS (**b**) solid-state NMR spectra of the non-functionalized (MSNs) and MPS surface functionalized samples via postsynthetic (MM1T) and co-condensation (MM-Co_{35}) routes

demonstrates that the arrangement of the characteristic structural units of amorphous silica is not distorted due to the bound silane functional groups and long modification process. For MSNs sample, two typical resonance signals of silica are well resolved at − 109.8 ppm and − 101.5 ppm which can be assigned to siloxane ($Si(SiO)_4$; Q^4) and free silanols ($SiOH(SiO)_3$; Q^3), respectively. A small signal is observed at − 92.0 ppm for geminal silanols ($Si(OH)_2(SiO)_2$; Q^2) (not shown in Fig. 3b). These signals are in agreement with the well-known and frequently reported chemical shift ranges of amorphous mesoporous silica (Zhao et al. 2001; Trébosc et al. 2005). The spectra show that the major part of the Si atoms exist as tetrahedral coordinated (Q^4) structure in addition to silicon atoms existing as the silanol groups (Q^3). The bulk consists of Q^4 species, whereas the surface contains OH groups mainly as Q^3 species. However, the samples treated with MPS (MM1T and MM-CO_{35}) display additional signals in the range from − 50 to − 70 ppm. The chemical shift corresponds the so-called mono-dental, bi-dental, or tri-dental structures: $SiR(OR')_2(OSi)$ (− 45 to − 50 ppm; T^1), $SiR(OR')(OSi)_2$ (− 55 to − 60 ppm; T^2), and $SiR(OSi)_3$ (− 60 to − 70 ppm; T^3), respectively, where R designates the organic functional groups of MPS ($((CH_2)_3CO_2(CH_3)C{=}CH_2$) and R′ is H or CH_3 (Bauer et al. 2000; Wei et al. 2012; Zúñiga et al. 2017). These new signals reveal that the silica surface is chemically modified without altering the original ordered mesopore structure in both functionalization methods. The ^{29}Si NMR results (Fig. 3b) revealed that the grafted alkoxysilanes are forming high proportions of T^2 and T^3 structures on the silica surface, which is in agreement with previous reports (Bauer et al. 2000; Rong et al. 2004; Wang et al. 2006). In our study, T^3 structures dominate on MM-Co_{35} sample prepared at basic condition in the presence of water and can only be explained by chemical grafting of pre-condensed MPS molecules (Bauer et al. 2003). The hydrolysis and self-condensation reactions of silanes are relatively suppressed in the postsynthetic modification route, under low water content (only physisorbed on the silica surface) and devoid of a catalyst. As a result, higher amount of T^2 species is formed compared with T^3 for MM1T sample (Fig. 3b). For reasons of simplicity and referring to the incomplete hydrolysis/condensation reactions, the bi-dental anchoring of MPS was considered to be representative for the reaction mechanism (Fig. 1) and for calculation purposes of silane grafting amount based on the TG and elemental analysis data (Table 1).

TG and elemental analyses

The silane grafting was quantitatively determined by TG and elemental analyses (Table 1). As shown in Fig. 4, the total weight loss of non-treated sample (MSNs) and silane-modified sample via the postsynthetic method in ethanol (MM1E) and toluene (MM1T) and for MM-Co_{35} sample was found 3, 11, 17, and 20%, respectively, in the range 200 to 800 °C. The percent weight loss in the ranges up to 200 °C, 200 to 400 °C, and 400 to 800 °C can be assigned to the vaporization of the physically adsorbed water and solvent, the thermo-oxidative degradation of the alkyl groups for a functionalized silica, and the condensation of surface hydroxyl groups from the unmodified or partially modified silica

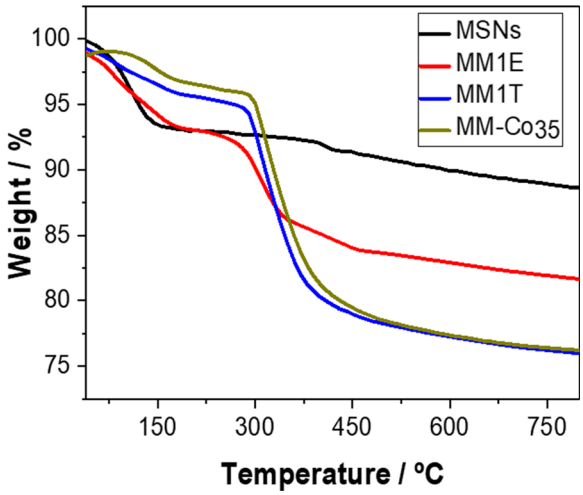

Fig. 4 TGA curve for non-functionalized (MSNs) and MPS functionalized silica samples via postsynthetic (MM1E and MM1T) and co-condensation (MM-Co_{35}) routes

surfaces, respectively (Ianchis et al. 2015). The recorded 3 wt% loss up to 800 °C for the MSN attributes to the removal of residue of organic components used for synthesis and the dehydration of the silica surface silanol groups, revealing its high thermal stability. The weight percent loss increased to 11%, 17%, and 20% for a sample modified using ethanol and, toluene and for MM-Co_{35} sample, respectively. This suggests the grafting and successive decomposition of more organic functional groups from MM-Co_{35} and MM1T samples than MM1E. The calculated actual weight percent loss of the bounded organic part on the silica surface in this study was found at 9, 14, and 17% for MM1E, MM1T, and MM-Co_{35} that infers the chemical grafting of acrylate groups on the silica surface.

The contents of acrylate groups on the final functionalized material were quantified based on the weight loss in the temperature range 200 to 800 °C from the TGA decomposition profile of the different materials prepared (Fig. 4). Alternative to the TGA, the silane amount was calculated based on the carbon content (wt% carbon) determined from elemental analysis. The external surface area of the as-synthesized MSNs sample (containing surfactant) was obtained from the BET method which is found equivalent to the values calculated from the *v-t* plot method (18 $m^2\ g^{-1}$). The grafting density calculated from both techniques is shown in Table 1. The carbon content for the MSNs sample (5.1%) arises due to the residues of organic precursors used for synthesis and has been subtracted from the carbon contents of the modified MSNs as presented in Table 1. The calculated surface coverage values for selected samples are in agreement in both analysis techniques. For modified samples prepared by the postsynthetic method, a very high grafting density was found for MM1T sample (31 and 29 molecules nm^{-2}) as well as MM1E (16 molecules nm^{-2}) from TGA and elemental analysis (Table 1). Ide et al. (2013) described that the contents of hydroxyl group in a fully hydroxylated silica surface were 4.2–5.7 OH groups nm^{-2}. The hydroxyl group density for the non-treated MSNs sample in the present work calculated from the TGA curve (Fig. 4) was found to be 3.4 OH groups nm^{-2}. Compared with hydroxyl group density, the final silane grafting density can be attributable to the grafting of self-precondensed silane oligomers on the external silica surface. In general, the results from FTIR, TG, and elemental analyses displayed toluene as the preferential solvent to achieve a high grafting density in the postsynthetic functionalization approach.

As demonstrated from CHN elemental analysis data of samples prepared via the co-condensation route, the time of silane addition during the silica framework formation influences the final silane content. Because of the relative homogenous grafting evidenced from N_2 sorption analysis, the silane content for MM-Co_5, MM-Co_{10}, and MM-Co_{20} samples was determined based on the total BET surface area. The calculated amount of silane was reduced sequentially as the time of silane addition is elongated from 5 (MM-Co_5) to 20 (MM-Co_{20}) minutes of ageing (Table 1). A maximum grafting amount of 1.7 molecules nm^{-2} was obtained for MM-Co_5 sample, which is close to the expected value (2 molecules nm^{-2}). The value was reduced to 0.9 molecules nm^{-2} for MM-Co_{20} sample. The low degree of surface coverage is attributed to the functionalization of part of the mesopore channels during the early stage of growth from initially formed oligosilicates in addition to the outer surface. However, this homogenous distribution is not highly pronounced for the sample prepared via incorporating the silane precursor to a fully grown material (MM-Co_{35}) where the silanes condense preferentially on the last layer of the particle surface. A sequential decrease in porosimetry values from the N_2 sorption analysis (Table 1) corresponding to the shortening of silane incorporation time from 35 to 5 min supports this explanation. Therefore, the

silane content of MM-Co_{35} sample in Table 1 was calculated based on the external surface area and found to be 39 and 40 molecules nm^{-2} from TGA and elemental analysis. This high grafting density is found due to the rapid hydrolysis and self-condensation of silanes in a highly basic aqueous conditions and bonding of large oligomers of silanes mainly as T^3 structure on the outer silica surface (Fig. 3b). Furthermore, the final loading of silane functional groups on the outer particle surface could be better controlled by adjusting the amount of silane precursor used in the modification solution in both modification methods.

SEM and TEM analyses

The SEM images (Fig. 5a–d) of selected MPS functionalized samples via postsynthetic (b: MM1T) and co-condensation (c: MM-Co_5 and d: MM-Co_{35}) methods indicated no significant change in morphology and dispersity compared with the non-treated sample (a: MSNs). Introducing the MPS during the early (MM-Co_5) or late stages (MM-Co_{35}) of particle growth neither affected the morphology nor the particle dispersity and size. However, the silane functionalization changed the surface properties of silica to be more hydrophobic. As a result, the dried particles are not easily dispersable in water, however well dispersed in a water/ethanol mixture. The average particle size of silane-functionalized samples determined from SEM micrographs using ImageJ software showed no significant variations (290 to 350 nm) compared with the non-treated sample (Table 1), designating that the introduction of the silanes via both routes had no paramount influence to the final morphological properties of the particles.

Well-defined spherical particles with an average particle size in the range of 290 to 345 nm are also observed from TEM analysis (Fig. 6a–d). A long-range pore ordering in the particles has been clearly observed for MM1T (b) and MM-Co_{35} (d) samples being analogous to the reference sample MSNs (a) as revealed from the TEM images. This result confirms that the periodicity of the pore structure is intact after the surface modification following both

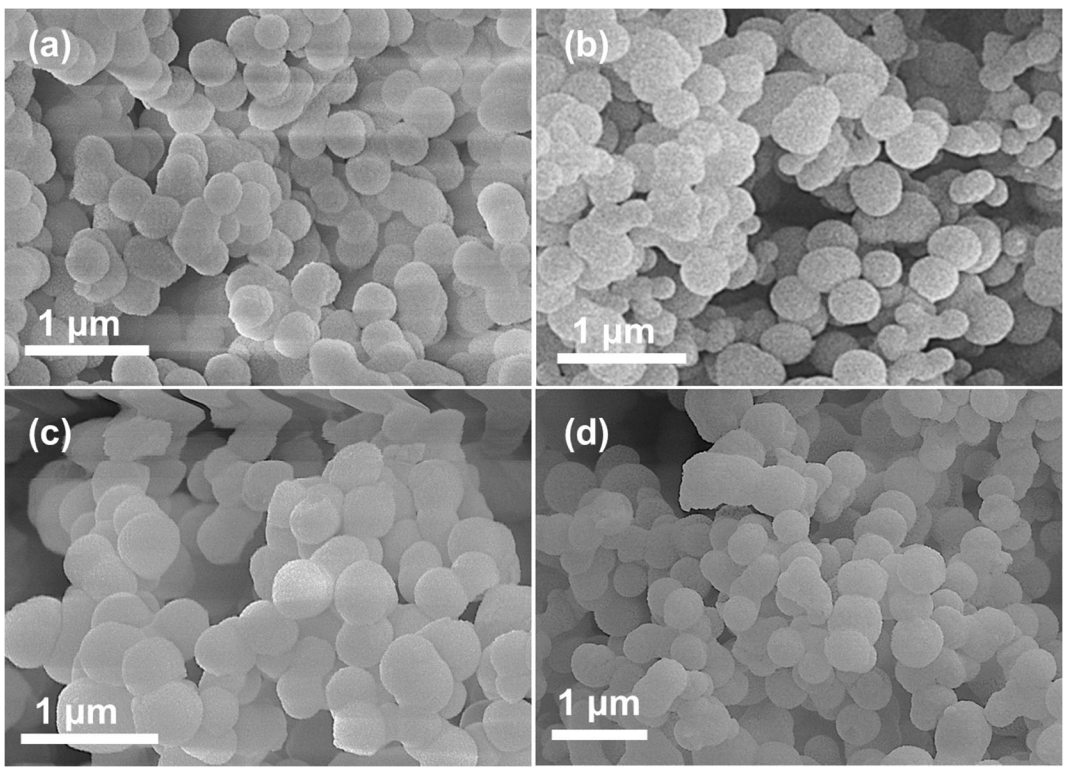

Fig. 5 SEM images of non-functionalized sample (MSNs: **a**) and silane functionalized samples via postsynthetic (MM1T: **b**) and co-condensation (MM-Co_5: **c** and MM-Co_{35}: **d**) routes

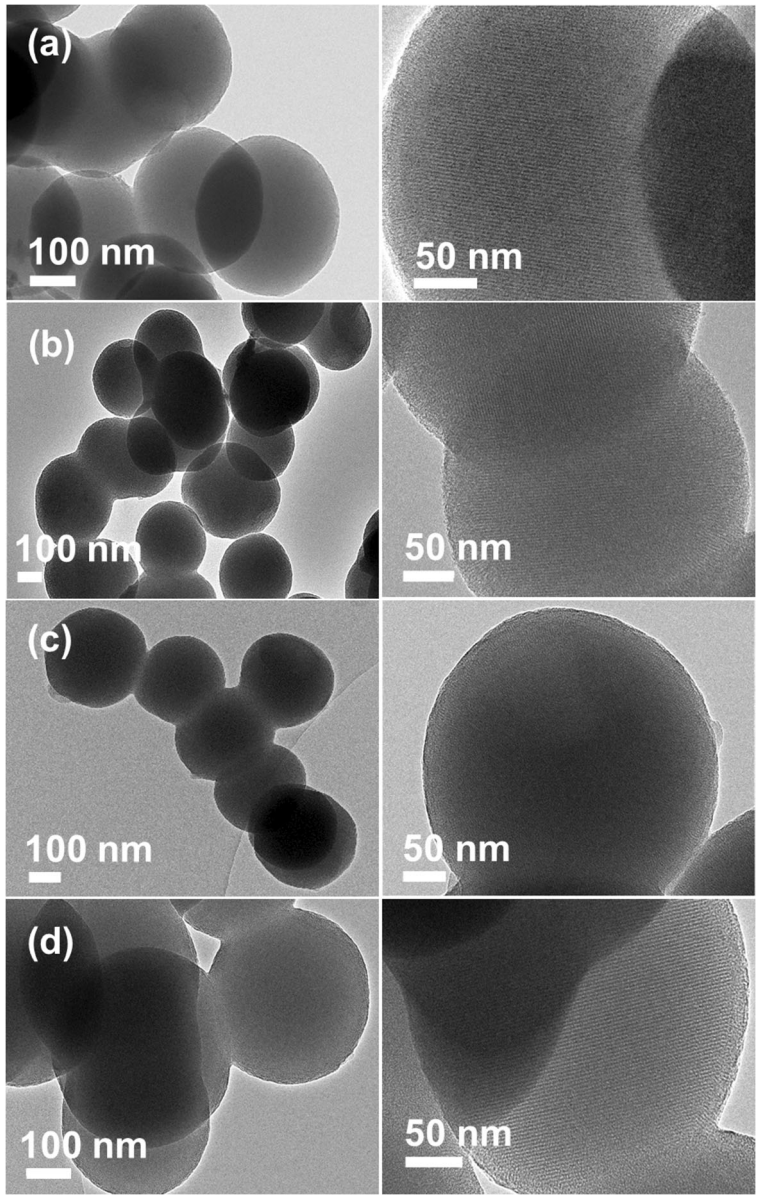

Fig. 6 TEM images of non-functionalized (MSNs: **a**) and silane functionalized samples via postsynthetic (MM1T: **b**) and co-condensation (MM-Co_5: **c** and MM-Co_{35}: **d**) pathways. The corresponding magnified images (right) with scale bar 50 nm for each figure show the pore structure

modification pathways. Overall, TEM analysis results are in agreement with SEM and XRD analysis techniques.

XRD and N_2 sorption analyses

The surface functionalization process has no destructive effect on the cubic mesopore structure of the particles prepared via both modification routes. The XRD patterns of MM1T with high surface coverage of acrylate species show well-resolved reflexes in the 2θ range of 2–6° corresponding to the lattice planes (211), (220), (420), and (332) (Fig. 7). The diffraction pattern, reflex intensity, and position are comparable to a typical highly ordered 3D MCM-48 cubic mesopore structure with the space group $Ia\bar{3}d$ of the non-functionalized sample (MSNs) (Solovyov et al. 2005; Yismaw et al. 2019). Therefore, the ordered cubic mesostructure was remained intact after a long postsynthetic process. Similarly, a comparable result was found for a sample prepared by incorporating the silane precursor to a fully grown particle (MM-Co_{35}) via the co-condensation approach. However, co-condensation during silica framework formation of the growing particles reveals slight

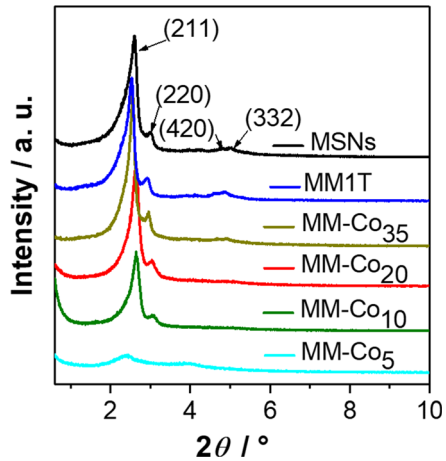

Fig. 7 XRD diffraction pattern of surface functionalized samples prepared by postsynthetic (MM1T) and co-condensation methods (MM-Co_5, MM-Co_{10}, MM-Co_{20}, MM-Co_{35}) compared with a non-modified sample (MSNs)

deviation depending on the time of silane addition. For MM-Co_{20} and MM-Co_{10} samples, the patterns at low-angle demonstrate two main reflexes related to (211) and (220) lattice planes, respectively, with a slight decrease in reflex intensity and reflex shift to higher 2θ value (Fig. 7), reflecting a slightly decreased length of the pore periodicity due to an earlier addition of the silane precursor. It is found that both functionalized MSNs samples composed of intact MCM-48-type cubic array of mesoporous channels. On the other hand, a successive decrease of the peak intensities for shorter ageing times before MPS addition reveals a distortion of the formation of the mesoporous framework. A single broad and low intense reflex related to (211) lattice planes is observed for MM-Co_5 sample (a sample prepared by adding the silane precursor during this early stage of silica framework formation). This suggests that the co-condensation of TEOS/silane during the very early stage of silica framework formation almost destructs the long-range cubic ordered mesopore structure.

The nitrogen sorption analysis of all samples (Figs. 8a and 9a) exhibits type IV isotherms being characteristic of high-quality mesoporous silica with the corresponding narrow pore width distribution determined from the NLDFT method (Yao et al. 2014). The porosimetry features of MM1E sample are less affected compared with MM1T sample showing a comparative reduction of the textural properties such as S_{BET} and V_{meso} (Table 1). As it was hypothesized, the template inside the pores and the reaction at room temperature limits the diffusion of the silane precursor into the pore channels and assists the preferential grafting of the silica oligomers formed on the outer surface of the nanoparticles. The silane oligomer grafting at the pore mouth could sterically hinder the complete access to the MSNs mesopore channels and block the pore entrance of sorbents (Bauer et al. 2004; Kecht et al. 2008; Zhao et al. 2011). Obviously, a more intense decrease in the S_{BET} and V_{meso} could be correlated with high grafting density using toluene as a solvent. This confirms the results of FTIR, TG, and elemental analyses. Thus, the solvent type has a significant effect on the final textural properties, content, and location of silane groups on MCM-48-

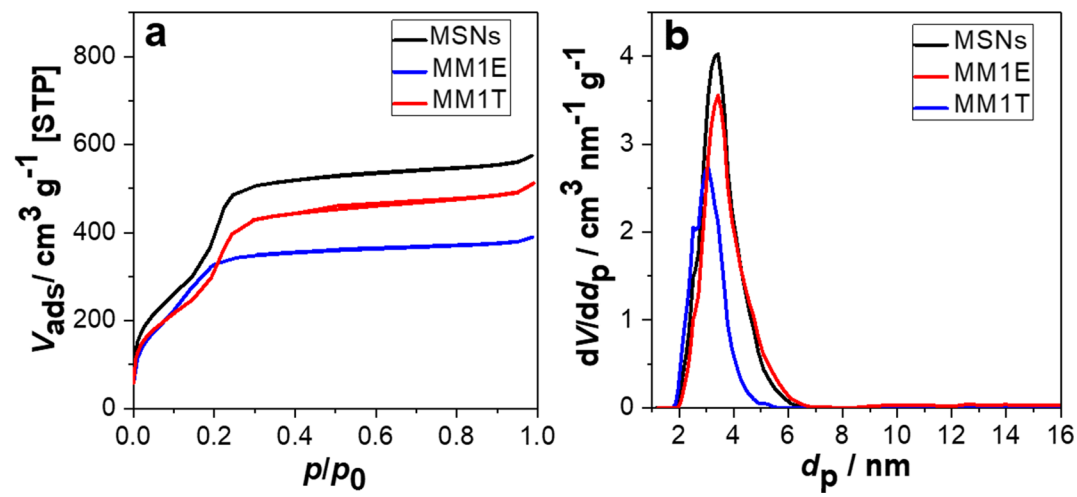

Fig. 8 N_2 sorption isotherms (**a**) and corresponding NLDFT pore width distributions (**b**) of non-functionalized (MSNs) and silane grafted silica samples using ethanol (MM1E) and toluene (MM1T)

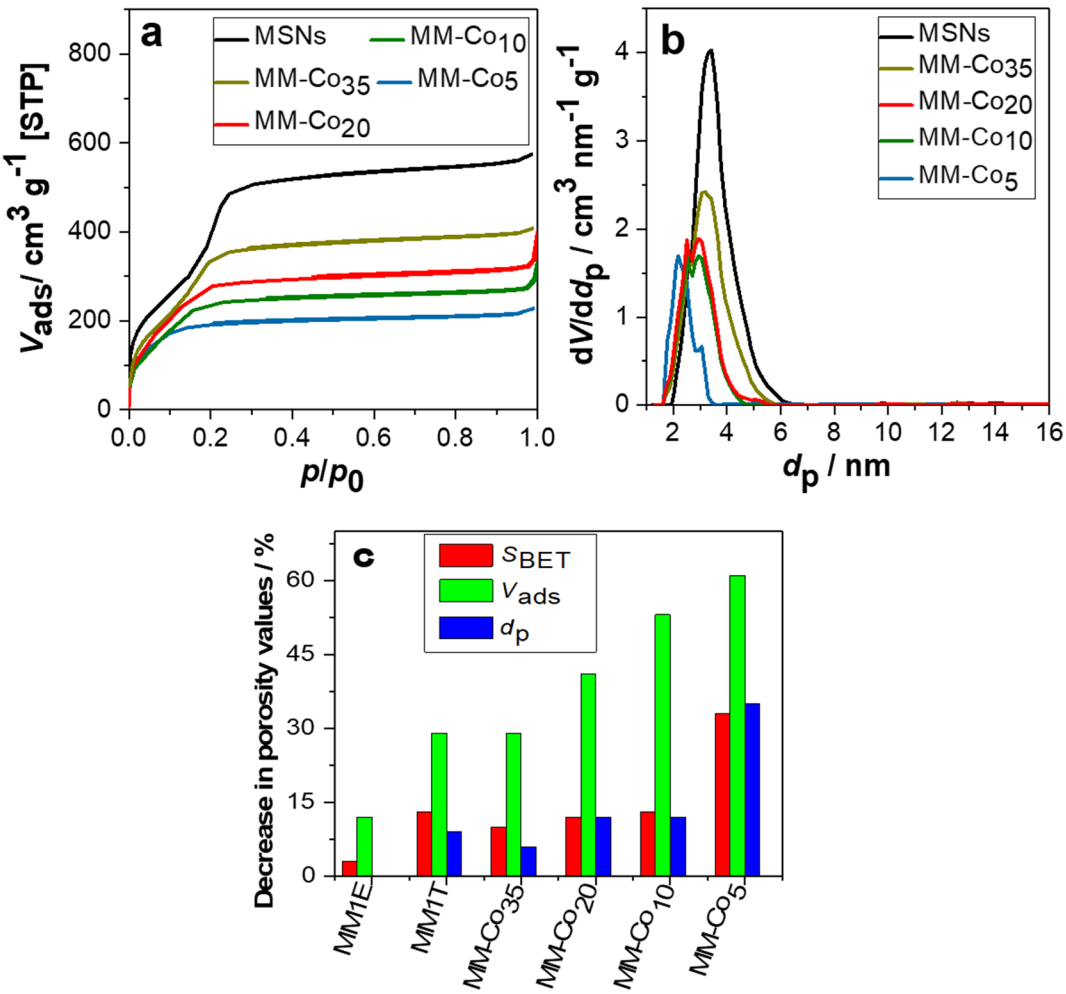

Fig. 9 (**a**) N_2 sorption isotherms and (**b**) NLDFT pore width distributions of surface functionalized samples prepared by the co-condensation method. (**c**) Quantitative data of porosimetry features: BET surface area (S_{BET}), total pore volume (V_{ads}), and NLDFT average pore diameter (d_p) decrease after surface modification

based nanoparticles. Based on the N_2 sorption analysis data, selective functionalization of the outer surface can be realized for MCM-48-type materials under the given optimal conditions as indicated by identical d_{meso}. This designates that the template inside the mesopores channels limits the diffusion of silane molecules into the 3D interconnected pore structure of MCM-48 silica.

For samples prepared by co-condensation processes, the BET surface area (S_{BET}), total pore volume (V_{ads}), and NLDFT average pore width (d_p) were reduced sequentially with regard to the addition time of silane (Fig. 9). The sample prepared at the early stage addition of silane (MM-Co_5) revealed a drastic decrease of S_{BET} (752 m^2 g^{-1}, 33%), V_{ads} (0.33 cm^3 g^{-1}, 61%) and d_p (2.2 nm, 35%) values compared with the non-treated silica sample (MSNs) (Fig. 9c). A homogenous distribution of the organosilane molecules partly occupying the mesopore channels during the silica framework formation results in a significant change in the textural properties. Moreover, an increase in loading of the incorporated organic groups can lead to a reduction in the pore diameter, pore volume, and specific surface area (Hoffmann et al. 2006). In the case of late addition of the silane species, the trialkoxysilanes hydrolyze rapidly under high basic conditions to give anionic species and later result in a high content of T^3 structures. The diffusion of the species into the pore channels is prevented by the template. These effects assist the selective functionalization of the outer surface during the particle growth (Kecht et al. 2008) via late silane

addition like MM-Co_{20} sample resulting in a decrease of 12% of S_{BET} and d_p, and 41% of V_{ads}. A highly selective functionalization of the outer particle surface with optimal textural properties and intact ordered MCM-48 pore structure MSNs was realized via late addition (after 35 min of ageing) of the silane precursor to a fully grown material (MM-Co_{35}). Barely, 10% of S_{BET}, 29% of V_{ads}, and 6% of d_p decrease were recorded for MM-CO_{35} sample (Fig. 9c). Overall, the time of silane addition to the reaction mixture alters the site selective binding process. The XRD and N_2 sorption results showed that an early MPS addition (MM-Co_5) leads to less organized pore networks. The porosimetry features and pore ordering are better preserved for samples prepared with late MPS additions (MM-Co_{10}, MM-Co_{20}, and MM-Co_{35}). In general, both MM1E, MM1T, and MM-Co_{35} samples selectively functionalized on the outer particle surface are characterized by optimal textural properties for any desire applications.

Conclusion

In the current study, MCM-48 silica nanoparticles functionalized on the outer surface with intact ordered mesopore structure and excellent textural and morphological properties are successfully synthesized in site selective manner for the first time. Our new optimized procedure, particularly the co-condensation modification route, represents a simple approach to synthesize structurally defined and site selective functionalized MCM-48 mesoporous silica materials in a one-step process. FTIR, ^{29}Si and ^{13}C solid-state NMR, TG, and elemental analysis measurements provide evidences for the successful chemical binding of silanes on silica surface. Highly site selective or more homogeneously distributed organic groups on the entire MCM-48-type silica surface were efficiently introduced by the co-condensation route at optimal reaction conditions. Late addition of the silane precursor to the batch of reaction mixture containing fully grown silica has no negative effect on the porosimetry data of the original material compared with the silane addition during the early stage of particle growth. A better control of outer surface functionalization was comprehended for already synthesized MCM-48 silica nanoparticles containing the template inside the pore channels at ambient temperature by the postsynthetic route. Moreover, a precise control of the loading of the outer surface with functional groups via reduction of the added amount of silanes for the postsynthetic modification or during later stages of the co-condensation process is the topic of our ongoing study.

The cubic ordered mesopore structure, textural properties, and morphology of the functionalized MCM-48 silica remain unaffected by the postsynthetic and co-condensation routes as evidenced from XRD, N_2 sorption, and electron microscope analyses. Both methods work efficiently to control the site selective silane grafting process on the outer surface of the silica nanoparticles preserving the necessary internal features for later applications as drug delivery systems after polymer grafting on the outer surface. Therefore, the synthesized nanoparticles with selectively functionalized outer surface in combination with optimal physicochemical properties are favorable candidates for subsequent site selective polymer grafting reactions.

Funding This research work was financially supported by the Institute of Chemical Technology, Faculty of Chemistry and Mineralogy, Universität Leipzig, and the German Academic Exchange Service (DAAD).

Compliance with ethical standards

Conflict of interest The authors declare that they have no conflict of interest.

References

Al-Oweini R, El-Rassy H (2009) Synthesis and characterization by FTIR spectroscopy of silica aerogels prepared using several $Si(OR)_4$ and $R''Si(OR')_3$ precursors. J Mol Struct 919: 140–145. https://doi.org/10.1016/j.molstruc.2008.08.025

Bartholome C, Beyou E, Bourgeat-Lami E, Chaumont P, Lefebvre F, Zydowicz N (2005) Nitroxide-mediated polymerization of styrene initiated from the surface of silica nanoparticles. In situ generation and grafting of alkoxyamine initiators. Macromolecules 38:1099–1106. https://doi.org/10.1021/ma048501i

Bauer F, Czihal S, Bertmer M, Decker U, Naumov S, Wassersleben S, Enke D (2017) Water-based functionalization of mesoporous siliceous materials, part 1: morphology and stability of grafted 3-aminopropyltriethoxysilane. Microporous Mesoporous Mater 250:221–231. https://doi.org/10.1016/j.micromeso.2016.01.046

Bauer F, Ernst H, Decker U, Findeisen M, Gläsel HJ, Langguth H, Hartmann E, Mehnert R, Peuker C (2000) Preparation of scratch and abrasion resistant polymeric nanocomposites by

monomer grafting onto nanoparticles, 1. FTIR and multinuclear NMR spectroscopy to the characterization of methacryl grafting. Macromol Chem Phys 201:2654–2659. https://doi.org/10.1002/1521-3935(20001201)201:18<2654::AID-MACP2654>3.0.CO;2-N

Bauer F, Ernst H, Hirsch D, Naumov S, Pelzing M, Sauerland V, Mehnert R (2004) Preparation of scratch and abrasion resistant polymeric nanocomposites by monomer grafting onto nanoparticles, 5. Macromol Chem Phys 205:1587–1593. https://doi.org/10.1002/macp.200400156

Bauer F, Sauerland V, Ernst H, Gläsel HJ, Naumov S, Mehnert R (2003) Preparation of scratch- and abrasion-resistant polymeric Nanocomposites by monomer grafting onto nanoparticles, 4. Macromol Chem Phys 204:375–383. https://doi.org/10.1002/macp.200390003

Bauer F, Sauerland V, Gläsel H-J, Ernst H, Findeisen M, Hartmann E, Langguth H, Marquardt B, Mehnert R (2002) Preparation of scratch and abrasion resistant polymeric Nanocomposites by monomer grafting onto nanoparticles, 3. Effect of filler particles and grafting agents. Macromol Mater Eng 287:546–552. https://doi.org/10.1002/1439-2054(20020801)287:8<546::AID-MAME546>3.0.CO;2-W

Biju V (2014) Chemical modifications and bioconjugate reactions of nanomaterials for sensing, imaging, drug delivery and therapy. Chem Soc Rev 43:744–764. https://doi.org/10.1039/C3CS60273G

Bouchoucha M, Côté M-F, C.-Gaudreault R et al (2016) Size-controlled functionalized mesoporous silica nanoparticles for tunable drug release and enhanced anti-tumoral activity. Chem Mater 28:4243–4258. https://doi.org/10.1021/acs.chemmater.6b00877

Chang B, Sha X, Guo J, Jiao Y, Wang C, Yang W (2011) Thermo and pH dual responsive, polymer shell coated, magnetic mesoporous silica nanoparticles for controlled drug release. J Mater Chem 21:9239–9247. https://doi.org/10.1039/c1jm10631g

Chen G, Zhou S, Gu G, Wu L (2007) Modification of colloidal silica on the mechanical properties of acrylic based polyurethane/silica composites. Coll Surf A Physicochem Eng Asp 296:29–36. https://doi.org/10.1016/j.colsurfa.2006.09.016

Doadrio JC, Sousa EMB, Izquierdo-Barba I, Doadrio AL, Perez-Pariente J, Vallet-Regí M (2006) Functionalization of mesoporous materials with long alkyl chains as a strategy for controlling drug delivery pattern. J Mater Chem 16:462–466. https://doi.org/10.1039/B510101H

Effati E, Pourabbas B (2012) One-pot synthesis of sub-50nm vinyl- and acrylate-modified silica nanoparticles. Powder Technol 219:276–283. https://doi.org/10.1016/j.powtec.2011.12.062

Feng J, Zhang H (2013) Hybrid materials based on lanthanide organic complexes: a review. Chem Soc Rev 42:387–410. https://doi.org/10.1039/C2CS35069F

Florea N-M, Lungu A, Vasile E, Iovu H (2013) The influence of nanosilica functionalization on the properties of hybrid nanocomposites. High Perform Polym 25:61–69. https://doi.org/10.1177/0954008312455831

He Q, Shi J, Zhu M, Chen Y, Chen F (2010) The three-stage in vitro degradation behavior of mesoporous silica in simulated body fluid. Microporous Mesoporous Mater 131:314–320. https://doi.org/10.1016/j.micromeso.2010.01.009

Hoffmann F, Cornelius M, Morell J, Fröba M (2006) Mesoporous silica-based organic-inorganic hybrid materials. Angew Chem 118:3290–3328. https://doi.org/10.1002/anie.200503075

Hui CM, Pietrasik J, Schmitt M, Mahoney C, Choi J, Bockstaller MR, Matyjaszewski K (2014) Surface-initiated polymerization as an enabling tool for multifunctional (nano-)engineered hybrid materials. Chem Mater 26:745–762. https://doi.org/10.1021/cm4023634

Ianchis R, Rosca ID, Ghiurea M, Spataru CI, Nicolae CA, Gabor R, Raditoiu V, Preda S, Fierascu RC, Donescu D (2015) Synthesis and properties of new epoxy-organolayered silicate nanocomposites. Appl Clay Sci 103:28–33. https://doi.org/10.1016/j.clay.2014.10.020

Ide M, El-Roz M, Canck ED et al (2013) Quantification of silanol sites for the most common mesoporous ordered silicas and organosilicas: total versus accessible silanols. Phys Chem Chem Phys 15:642–650. https://doi.org/10.1039/C2CP42811C

Jin X, Wang Q, Sun J, Panezai H, Bai S, Wu X (2017) Dual (pH- and temperature-) stimuli responsive nanocarrier with bimodal mesoporous silica nanoparticles core and copolymer shell for controlled ibuprofen-releasing: fractal feature and diffusion mechanism. Microporous Mesoporous Mater 254:77–85. https://doi.org/10.1016/j.micromeso.2017.05.003

Kecht J, Schlossbauer A, Bein T (2008) Selective functionalization of the outer and inner surfaces in mesoporous silica nanoparticles. Chem Mater 20:7207–7214. https://doi.org/10.1021/cm801484r

Khosraviyan P, Ardestani MS, Khoobi M et al (2016) Mesoporous silica nanoparticles functionalized with folic acid/methionine for active targeted delivery of docetaxel. Onco Targets Ther 9:7315–7330. https://doi.org/10.2147/OTT.S113815

Léonard A, Dandoy P, Danloy E, Leroux G, Meunier CF, Rooke JC, Su BL (2011) Whole-cell based hybrid materials for green energy production, environmental remediation and smart cell-therapy. Chem Soc Rev 40:860–885. https://doi.org/10.1039/c0cs00024h

Luan Z, Fournier JA, Wooten JB et al (2005) Functionalized mesoporous SBA-15 silica molecular sieves with mercaptopropyl groups: preparation, characterization and application as adsorbents. Stud Surf Sci Catal 156:897–906. https://doi.org/10.1016/S0167-2991(05)80302-7

Mamaeva V, Sahlgren C, Lindén M (2013) Mesoporous silica nanoparticles in medicine–recent advances. Adv Drug Deliv Rev 65:689–702. https://doi.org/10.1016/j.addr.2012.07.018

Marini M, Pourabbas B, Pilati F, Fabbri P (2008) Functionally modified core-shell silica nanoparticles by one-pot synthesis. Colloids Surfaces A Physicochem Eng Asp 317:473–481. https://doi.org/10.1016/j.colsurfa.2007.11.022

Morelli C, Maris P, Sisci D, Perrotta E, Brunelli E, Perrotta I, Panno ML, Tagarelli A, Versace C, Casula MF, Testa F, Andò S, Nagy JB, Pasqua L (2011) PEG-templated mesoporous silica nanoparticles exclusively target cancer cells. Nanoscale 3:3198–3207. https://doi.org/10.1039/c1nr10253b

Pardal F, Lapinte V, Robin J-J (2009) Modification of silica nanoparticles by grafting of copolymers containing organosilane and fluorine moities. J Polym Sci Part A Polym Chem 47:4617–4628. https://doi.org/10.1002/pola.23513

Perissinotto AP, Awano CM, Donatti DA, de Vicente FS, Vollet DR (2015) Mass and surface fractal in supercritical dried silica aerogels prepared with additions of sodium dodecyl sulfate. Langmuir 31:562–568. https://doi.org/10.1021/la504272g

Pinto PR, Mendes LC, Dias ML, Azuma C (2006) Synthesis of acrylic-modified sol–gel silica. Colloid Polym Sci 284:529–535. https://doi.org/10.1007/s00396-005-1424-0

Rong MZ, Zhang MQ, Pan SL, Friedrich K (2004) Interfacial effects in polypropylene-silica nanocomposites. J Appl Polym Sci 92:1771–1781. https://doi.org/10.1002/app.20139

Solovyov LA, Belousov OV, Dinnebier RE, Shmakov AN, Kirik SD (2005) X-ray diffraction structure analysis of MCM-48 Mesoporous silica. J Phys Chem B 109:3233–3237. https://doi.org/10.1021/jp0482868

Subagyono DJN, Marshall M, Knowles GP, Chaffee AL (2014) CO_2 adsorption by amine modified siliceous mesostructured cellular foam (MCF) in humidified gas. Microporous Mesoporous Mater 186:84–93. https://doi.org/10.1016/j.micromeso.2013.11.032

Sun Y, Zhang Z, Wong CP (2005) Study on mono-dispersed nano-size silica by surface modification for underfill applications. J Colloid Interface Sci 292:436–444. https://doi.org/10.1016/j.jcis.2005.05.067

Tang L, Casas J, Venkataramasubramani M (2013) Magnetic nanoparticle mediated enhancement of localized surface plasmon resonance for ultrasensitive bioanalytical assay in human blood plasma. Anal Chem 85:1431–1439. https://doi.org/10.1021/ac302422k

Tarn D, Ashley CE, Xue M, Carnes EC, Zink JI, Brinker CJ (2013) Mesoporous silica nanoparticle nanocarriers: biofunctionality and biocompatibility. Acc Chem Res 46:792–801. https://doi.org/10.1021/ar3000986

Trébosc J, Wiench JW, Huh S, Lin VSY, Pruski M (2005) Solid-state NMR study of MCM-41-type mesoporous silica nanoparticles. J Am Chem Soc 127:3057–3068. https://doi.org/10.1021/ja043567e

Trewyn BG, Giri S, Slowing II, Lin VS-Y (2007) Mesoporous silica nanoparticle based controlled release, drug delivery, and biosensor systems. Chem Commun 38:3236–3245. https://doi.org/10.1039/b701744h

Tsai C-P, Chen C-Y, Hung Y, Chang FH, Mou CY (2009) Monoclonal antibody-functionalized mesoporous silica nanoparticles (MSN) for selective targeting breast cancer cells. J Mater Chem 19:5737–5743. https://doi.org/10.1039/b905158a

Vashist SK, Lam E, Hrapovic S, Male KB, Luong JHT (2014) Immobilization of antibodies and enzymes on 3-aminopropyltriethoxysilane-functionalized bioanalytical platforms for biosensors and diagnostics. Chem Rev 114:11083–11130. https://doi.org/10.1021/cr5000943

Villenas I, Rivas BL, Torres C, Campos C, Urbano BF (2015) Effect of functionalized trititanate nanotubes on the properties of crosslinked cationic polymer nanocomposite. Polym Int 64:1121–1127. https://doi.org/10.1002/pi.4874

Wang K, He X, Yang X, Shi H (2013) Functionalized silica nanoparticles: a platform for fluorescence imaging at the cell and small animal levels. Acc Chem Res 46:1367–1376. https://doi.org/10.1021/ar3001525

Wang Y, Li Y, Zhang R, Huang L, He W (2006) Synthesis and characterization of nanosilica/polyacrylate composite latex. Polym Compos 27:282–288. https://doi.org/10.1002/pc.20200

Wei L, Shi D, Zhou Z, Ye P, Wang J, Zhao J, Liu L, Chen C, Zhang Y (2012) Functionalized self-assembled monolayers on mesoporous silica nanoparticles with high surface coverage. Nanoscale Res Lett 7:334. https://doi.org/10.1186/1556-276X-7-334

Yao M, Dong Y, Feng X, Hu X, Jia A, Xie G, Hu G, Lu J, Luo M, Fan M (2014) The effect of post-processing conditions on aminosilane functionalizaiton of mesocellular silica foam for post-combustion CO_2 capture. Fuel 123:66–72. https://doi.org/10.1016/j.fuel.2014.01.059

Yismaw S, Kohns R, Schneider D, Poppitz D, Ebbinghaus SG, Gläser R, Tallarek U, Enke D (2019) Particle size control of monodispersed spherical nanoparticles with MCM-48-type mesostructure via novel rapid synthesis procedure. J Nanopart Res 21:258. https://doi.org/10.1007/s11051-019-4699-7

Zamboulis A, Moitra N, Moreau JJE, Cattoën X, Wong Chi Man M (2010) Hybrid materials: versatile matrices for supporting homogeneous catalysts. J Mater Chem 20:9322–9338. https://doi.org/10.1039/c000334d

Zhao H, Ma Y, Tang J, Hu J, Liu H (2011) Influence of the solvent properties on MCM-41 surface modification of aminosilanes. J Solut Chem 40:740–749. https://doi.org/10.1007/s10953-011-9685-3

Zhao W, Luo Y, Deng P, Li Q (2001) Synthesis of Fe-MCM-48 and its catalytic performance in phenol hydroxylation. Catal Lett 73:199–202. https://doi.org/10.1023/A:1016674605967

Zimmermann Y, Anders S, Hofmann K, Spange S (2002) Influence of chemical solvent properties on the external and internal surface polarity of silica particles in slurry. Langmuir 18:9578–9586. https://doi.org/10.1021/la020574c

Zúñiga E, Belmar L, Toledo L, Torres C, Rivas BL, Sánchez SA, Urbano BF (2017) Rhodamine-loaded surface modified mesoporous silica particles embedded into a thermoresponsive composite hydrogel for prolonged release. Eur Polym J 95:358–367. https://doi.org/10.1016/j.eurpolymj.2017.08.018